Applied Radiation and Isotopes 69 (2011) 1858–1861

Contents lists available at ScienceDirect

Applied Radiation and Isotopes

journal homepage: www.elsevier.com/locate/apradiso

First tomographic image of neutron capture rate in a BNCT facility

D.M. Minsky [a,b,c,*], A.A. Valda [a,b], A.J. Kreiner [a,b,c], S. Green [d,e], C. Wojnecki [d,e], Z. Ghani [e]

[a] Gerencia de Investigación y Aplicaciones, CAC, CNEA, Av. Gral. Paz 1499 (B1650KNA), San Martín, Prov. Bs. As., Argentina
[b] Escuela de Ciencia y Tecnología, , UNSAM, M. de Irigoyen 3100 (1650), San Martín, Prov. Bs. As., Argentina
[c] Conicet, Av. Rivadavia 1917 (C1033AAJ), Buenos Aires, Argentina
[d] School of Physics and Astronomy, University of Birmingham, B15 2 TT, UK
[e] Department of Medical Physics, University Hospital Birmingham, Birmingham B15 2TH, UK

ARTICLE INFO

Available online 1 February 2011

Keywords:
SPEC
BNCT dosimetry
Boron dose

ABSTRACT

This work discusses the development of online dosimetry of the boron dose via Single Photon Emission Computed Tomography (SPECT) during a BNCT treatment irradiation. Such a system will allow the online computation of boron dose maps without the large current uncertainties in the assessment of the boron concentration in different tissues. The first tomographic boron dose image with a SPECT prototype is shown.

1. Introduction

In Boron Neutron Capture Therapy (BNCT) the dose delivered to healthy and tumor tissues depends on the interactions of neutrons with many different nuclei and the gamma ray background. In the tumor and with current ^{10}B concentrations, about 80% of the dose is due to neutron captures in boron (boron dose). Boron dose depends not only on the neutron field but also on the distribution of boron among different tissues. Nowadays, the boron dose is estimated by simulations and measurements to assess the neutron field convoluted with estimations on the boron concentrations. Boron concentration distributions are inferred based on blood samples taken before, during and after the patient irradiation, and previous statistical studies, which relate boron concentration in different tissues with boron concentration in blood. Patient-to-patient differences lead to big uncertainties in this biodistribution studies and these uncertainties are reflected in the dosimetry with current methods.

In 94% of the cases after neutron capture in ^{10}B, the residual ^{7}Li nucleus is emitted in its first excited state and promptly decays via a characteristic 478 keV gamma ray. The attenuation coefficient for this photon in soft tissue is about 0.1 cm^{-1} and hence it can escape from the patient's body and can be detected as a measure of the boron dose. Verbakel and Stecher-Rasmussen (1997), (2001) have constructed a device named Gamma Ray Telescope for the determination of boron dose by the detection of this gamma ray and with some geometrical assumptions on the body's shapes. Kobayashi et al. (2000) have made a feasibility analysis of a SPECT for the quantification of the boron dose. AfRosenschöld (2006) have measured the 478 keV prompt gammas coming from a phantom in order to develop the tomography but the background contamination was very high and they finally used a phantom loaded with a gamma emitter to obtain a standard SPECT image that does not represent the problems of the complex neutron and gamma field present in BNCT. We have worked both numerically and experimentally in the development of a SPECT system for obtaining boron dose maps during a BNCT irradiation (Minsky et al., 2006, 2009).

In the present work we show experimental results on the acquisition of the first SPECT map of neutron captures in boron rate, which is directly related to the boron dose.

2. Materials and methods

A SPECT prototype for online boron dose map measurements has been constructed. The prototype consists of four $LaBr_3(Ce)$ scintillators with their collimators, shielding and displacement system. The lead collimators are 0.5 cm in diameter and 30 cm in length. The shielding has been constructed of successive layers, from outside to inside: a layer of a mixture of paraffin and lithium carbonate to moderate and absorb neutrons; a cadmium layer for further shielding of thermal neutrons; a lead layer for shielding gammas and a final layer of lithium carbonate enriched in ^{6}Li for absorbing the remaining thermal neutrons. The SPECT prototype was mounted on motorized rails that allowed to place the collimators on all bin positions. In our approach, a full projection

* Corresponding author at: Gerencia de Investigación y Aplicaciones, CAC, CNEA, Av. Gral. Paz 1499 (B1650KNA), San Martín, Prov. Bs. As., Argentina.
Tel.: +54 11 6772 7913; fax: +54 11 6772 7121.
E-mail address: minsky@tandar.cnea.gov.ar (D.M. Minsky).

0969-8043/$ - see front matter © 2011 Elsevier Ltd. All rights reserved.
doi:10.1016/j.apradiso.2011.01.030

set consists of 41 bins, and a full acquisition consists in 20 projections.

A 9 cm radius water filled cylindrical head phantom with a 3 cm diameter cylindrical tumor model with 400 ppm of ^{10}B was used for the experiments. The phantom was positioned at the Birmingham University accelerator based BNCT facility (Culbertson et al., 2004) and irradiated with the accelerator set at 800 μA and 2.8 MeV. In order to measure different projections and instead of rotating the detection system, the phantom was rotated around its axis; this rotation, the detector displacement movements and all the measurements were made in a computer controlled way.

In order to avoid energy drifts along the measurements, all spectra have been re-calibrated in energy by fitting the 511 keV pair annihilation and 2223 keV peaks from neutron absorptions in hydrogen before further analysis. Expectation Maximization–Maximum Likelihood algorithm (Shepp and Vardi, 1982) was implemented in C language for the reconstruction of the image.

Neutron and photon transport simulations have been performed with the MCNP 5 1.40 code (Brown et al. 2002). The simulations model all the moderation and conformation processes in the beam shaping assembly, the interactions inside the phantom and the effects on the SPECT prototype.

3. Results and discussion

The measured spectra show a high gamma ray background. The most pronounced peaks come from pair annihilation and neutron captures in hydrogen (Fig. 1). Although the ^{10}B neutron capture 478 keV peak was small compared to the 511 keV pair annihilation peak, the differences in count rate of measurements with collimators pointing to tumor and pure water zones could be distinguished (Fig. 2). In order to accurately calculate the 478 keV peak areas, both peaks have been taken into account in a fitting process of the spectra. This fitting has been made considering two Gaussian peaks and an exponential background.

MCNP simulations show very good agreement with measured neutron capture in boron peak areas. The simulations take into account all the neutron and photon transports in the beam shaping assembly, phantom, collimators, and detector shielding. The detector intrinsic efficiency was measured and added as a multiplying factor to the simulations. As an example, Fig. 3 shows the comparison of measurements and simulations for one projection.

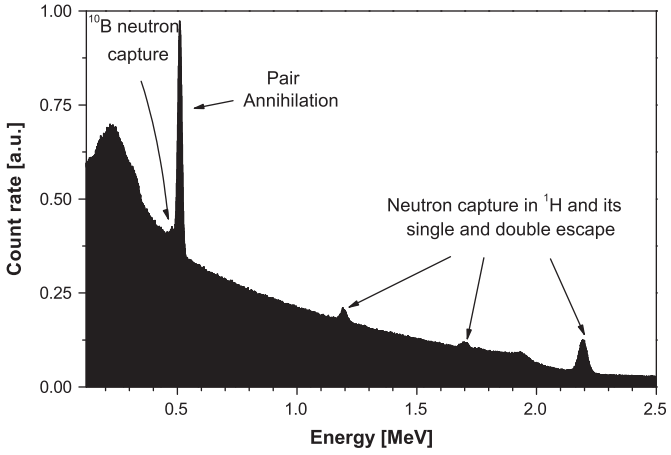

Fig. 1. Gamma ray spectrum shows very prominent ^{1}H neutron capture and pair annihilation peaks and a weak ^{10}B neutron capture peak.

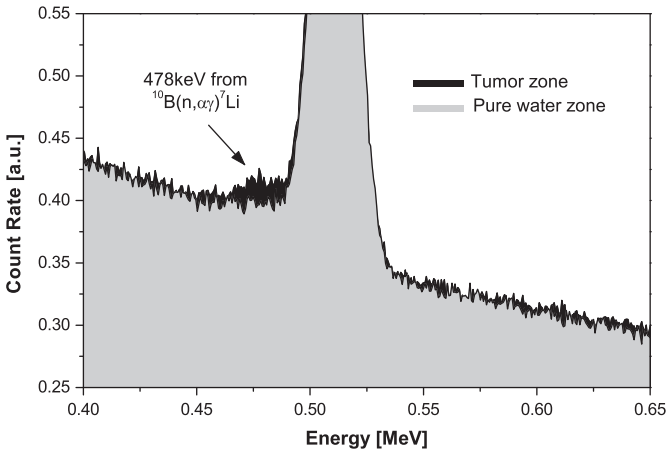

Fig. 2. Gamma ray spectrum showing the small measured difference pointing the collimators to a pure water zone and to a tumor zone.

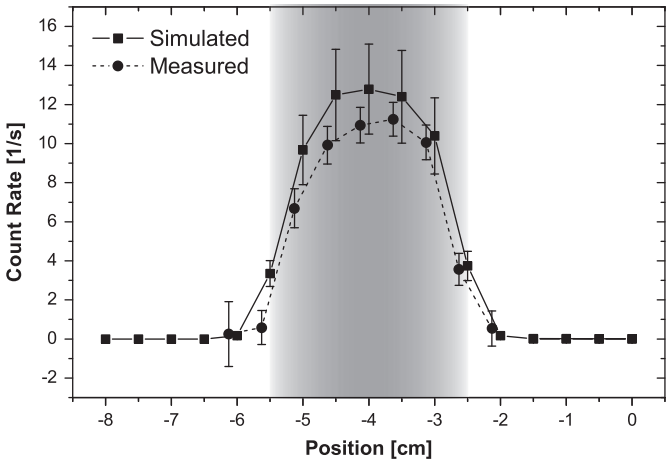

Fig. 3. Simulated and measured comparison of one projection. The shaded region indicates the tumor position.

All the spectra were measured for 20 min periods, this correspond to about 10% of the irradiation time of a BNCT treatment with this facility operating at a proton current of 800 μA. A total of 7 projections were measured and symmetries were exploited to complete a total of 13 projections. In the original design a total of 20 projections to be measured were proposed, but for this feasibility test 13 were considered sufficient. In case of a complete tomographic system with enough detectors to measure 3 complete projections simultaneously, all the acquisitions for a tomography could be done during a treatment time.

The system could reconstruct a 21×21 pixels of 1 cm $\times$ 1 cm size image map of neutron capture in boron density rate (Figs. 4 and 5). The reconstructed neutron capture in boron rate density with the experimental measurements is $1.7 \times 10^{7}\,s^{-1}\,cm^{-3}$(error $\sim$15%) at the central pixel of the image and the simulated by MCNP5 is $1.75 \times 10^{7}\,s^{-1}\,cm^{-3}$ (error $<1\%$), both results agree within errors.

The neutron dose map could be reconstructed with a tumor model with boron concentration a factor of 8 bigger than concentrations that can be actually reached with current boron delivery agents. Thus one should analyze if the reconstruction would be possible in a realistic situation. Previous statistical analysis (Minsky, 2008) shows that the error in the reconstructed rate depends on the most significant bin measured on all projections. In the experiment shown, this bin corresponds to the one that sees the tumor along its diameter and the experimental

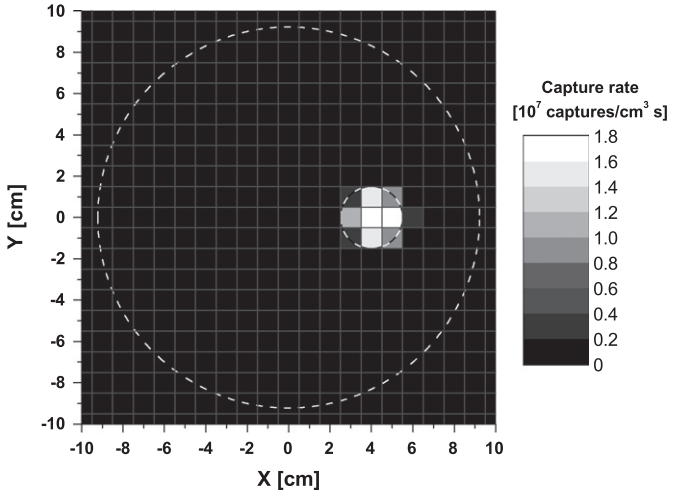

Fig. 4. Reconstructed neutron capture in boron density rate map. The dotted circles indicate the phantom and the tumor boundaries.

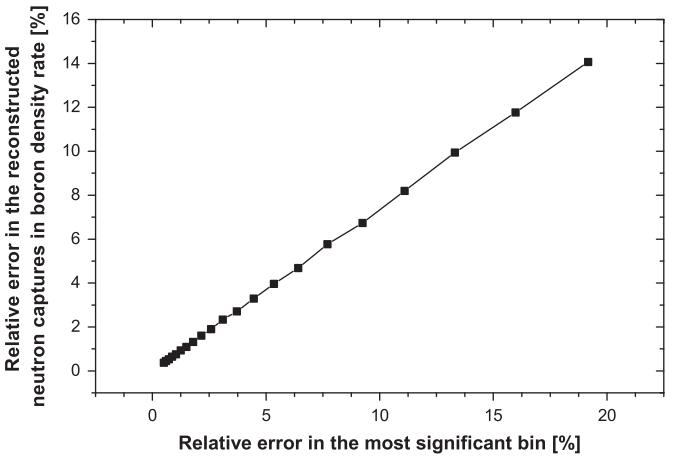

Fig. 6. Relative error in the reconstructed neutron capture density rate as function of the relative error in the most significant bin.

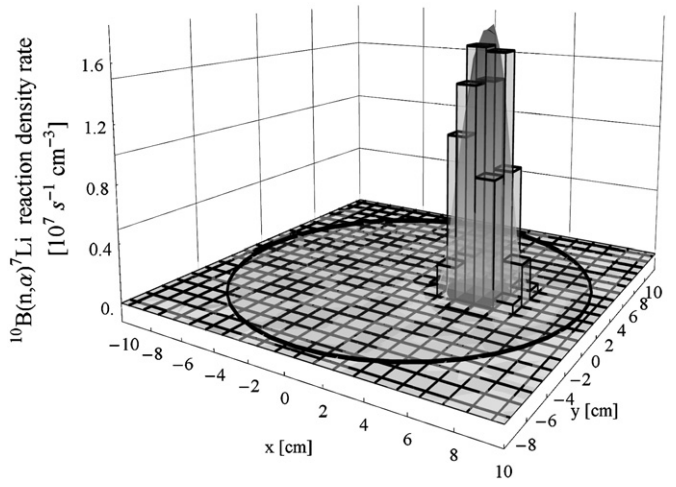

Fig. 5. Reconstructed neutron capture in boron density rate map. The bars represent the reconstructed data and the shaded curve an interpolation. The circles on the base indicate the phantom and the tumor boundaries.

relative error for that bin is 8%. In the case of a full set of 20 projections, the reconstructed relative error is about 70% of the error in the most significant bin (Fig. 6), so the reconstructed error would be 5.5%. Thus if one accepts errors of 20%, 4 times larger, acquisition times can be reduced by a factor of 16. It is not possible to say that with the same acquisition time the boron concentration in the tumor model can be reduced by the same factor since the background would remain constant, but this concentration can probably be considerably reduced.

In the case of the experiment we have measured only 7 independent projections, so the resulting error is 15%. In the experiments there was boron only in the tumor, if we distribute the same amount of boron along the line seen by the most significant detector keeping the 4:1 ratio between tumor and healthy tissues, this will make concentration of about 60 ppm in healthy tissue and 240 ppm in tumor.

Standard 1 in. $\times$ 1 in. cylindrical crystal scintillators have been used in this prototype. As the collimator holes are 0.5 cm in diameter, the total volume of the detector material can be dramatically reduced as the front face is matched to the 0.5 cm diameter. The detector depth can also be increased. After adapting the detector geometry, the crystal thickness in the direction of photons coming from the collimator would increase and so will the intrinsic efficiency. On the other hand the thickness for photons impinging laterally will diminish dramatically so the detector would have much less intrinsic efficiency for the gamma background that comes from directions other than the collimator holes. An improvement in the sensitivity of the neutron capture in boron peak and in the signal to noise ratio will thus allow lower detection limits and lower measuring times.

4. Conclusions

The first tomographic image of the boron dose of a phantom irradiated at a facility with a clinical BNCT neutron spectrum has been obtained. The experimentally reconstructed neutron capture rate density in the tumor and the simulated one agree within errors.

Further work should be done in order to reduce the background and in detector optimization for detection limit improvement. Dedicated detectors and a better shielding should let achieve the goal of 20% in the error measuring projections of tumors with 40 ppm and thus allowing to reconstruct boron dose images with 15% error.

This work shows that SPECT images based on the detection of the 478 keV capture gamma ray is a promising option for BNCT dosimetry that does not undergo the problem of the assessment of the boron distribution of current methods.

Acknowledgment

A grant from the Agencia Nacional de Promocion Cientifica y Tecnologica, PAV 22619, is acknowledged.

References

AfRosenschöld, P.M., 2006. Prompt gamma tomography during BNCT—a feasibility study. J. Instrum. 1, 1–10.

Brown, F., et al., 2002. MCNP version 5, LA-UR-02-3935 Tech. Rep., Los Alamos National Laboratory.

Culbertson, C.N., et al., 2004. In-phantom characterisation studies at the Birmingham Accelerator-Generated epIthermal Neutron Source (BAGINS) BNCT facility. Appl. Radiat. Isot. 61 (5), 733–738.

Kobayashi, T., et al., 2000. A noninvasive dose estimation system for clinical BNCT based on PG-SPECT- Conceptual study and fundamental

experiments using HPGe and CdTe semiconductor detectors. Med. Phys. 27, 2124–2132.
Minsky, D.M., et al., 2006. Design of a SPECT tomographic image system for online dosimetry in BNCT. Advances in Neutron Capture Therapy 2006. International Society for Neutron Capture Therapy, 405–408.
Minsky, D.M., 2008. Ph.D. Thesis, Buenos Aires University.
Minsky, D.M., et al., 2009. Experimental feasibility studies on a SPECT tomograph for BNCT dosimetry. Appl. Radiat. and Isot. 67, s179–s182.
Shepp, L.A., Vardi, Y., 1982. Maximum likelihood reconstruction for emission tomography. IEEE Trans. Nucl. Imaging 1, 113–122.
Verbakel, W.F.A.R., Stecher-Rasmussen, F., 1997. A gamma-ray telescope for on-line measurements of low boron concentrations in a head phantom for BNCT. Nucl. Instrum. Methods Phys. Res. A 394, 163–172.
Verbakel, W.F.A.R., Stecher-Rasmussen, F., 2001. On-line reconstruction of low boron concentrations by in vivo gamma-ray spectroscopy for BNCT. Phys. Med. Biol. 46, 687–701.